International Journal of Technology

http://ijtech.eng.ui.ac.id

Research Article

The Influence of Thermal and Mechanical Loads on The Piston when the Engine Operates on CNG Fuel is Assessed

Nguyen Duy Tien[1], Nguyen Van Tuan[2*]

[1]The School of Mechanical Engineering, Hanoi University of Science and Technology, No. 1 Dai Co Viet Street, Bach Mai Ward, Hanoi 100000, Vietnam

[2]Mechanical Power Engineering and Automation research group, University of Transport Technology, Hanoi 100000, Vietnam

[*]Corresponding author: nguyenvantuan@utt.edu.vn; Tel.: +84982647320; Fax.: +84243854 7695

Abstract: This study numerically simulates the mechanical and thermal durability of a diesel engine piston after conversion to compressed natural gas (CNG) operation. Combustion cycle simulations indicate that the peak pressure and temperature increase by 37.44% and 2%, respectively, when using CNG, thereby altering the piston's operating conditions. The analysis results show a significant reduction in mechanical loading, with maximum stress and deformation decreasing by 45% and 43.75%, respectively, compared with diesel operation. In contrast, thermal loading increases, leading to a corresponding rise of 5% and 4% in thermal stress and thermal deformation, respectively. Under combined loading, the total stress decreases slightly by 5%, whereas the total deformation increases by 8%, reflecting the high-temperature but low-pressure combustion characteristics of CNG. Although the piston remains within allowable operating limits, thermal loading is identified as the dominant factor governing failure risk. These findings provide essential technical insights for optimizing piston design and cooling systems to enhance the reliability of CNG-converted engines.

Keywords: CNG fuel; Internal combustion engine; Mechanical load; Thermal load

1. Introduction

In conventional diesel engines, extensive research has been conducted to identify effective approaches for reducing fuel consumption and limiting pollutant emissions. Recent studies indicate that compressed natural gas–diesel dual-fuel engines represent a promising short- and medium-term solution for improving energy efficiency and mitigating harmful emissions (Kyando et al., 2026; Kundu and Gupta, 2024; Nsaif et al., 2024). In addition, the potential of CNG as an alternative fuel for conventional internal combustion engines has been explored in several studies (Ali et al., 2024; Meng et al., 2019). Compressed natural gas is widely recognized as a relatively clean fuel with a high octane number, enabling engines to operate at higher compression ratios. Moreover, it mixes effectively with air, promoting a more homogeneous combustion process and consequently reducing pollutant formation (Karczewski and Wieczorek, 2021; Yousefi et al., 2019). Furthermore, both experimental and numerical studies have demonstrated that fuel injection conditions, combustion chamber geometry, and in-cylinder flow behavior strongly influence the combustion characteristics and performance of dual-fuel engines (Shen et al., 2021; Cihan et al., 2020).

When a diesel engine is converted to operate with compressed natural gas (CNG), its operating characteristics may change considerably. In many cases, the engine power output may improve, while the mechanical load acting on the piston tends to decrease. However, piston temperatures may increase significantly and can exceed 400°C, which could reduce structural durability if appropriate cooling strategies are not implemented (Qi et al., 2021; Wang et al.,

https://doi.org/10.14716/ijtech.v17i3.8315
Received December 2025; Revised February 2026; Accepted April 2026

2019). Therefore, evaluating the piston's strength and reliability under CNG operating conditions is of considerable importance. The piston is one of the key components in internal combustion engines responsible for energy conversion. The connecting rod transfers the energy generated during the combustion of the air–fuel mixture to the crankshaft and is subjected to extremely high pressures and temperatures during operation (Liu et al., 2023; Zhang et al., 2019). In addition to transmitting force, it helps maintain combustion chamber sealing and facilitates heat transfer to the engine cooling system (Sadiq and Iyer, 2020). Modern piston design aims to achieve an optimal balance between mechanical strength, thermal resistance, and lightweight characteristics. Numerous studies have focused on improving piston geometry, material selection, and numerical simulation techniques, such as finite element analysis (FEA), to evaluate piston stress and deformation under various operating conditions (Lei et al., 2024; Chen et al., 2020). Computational fluid dynamics and heat-transfer models have been widely applied to investigate thermal exchange processes within engines (Plotnikov, 2024; Du et al., 2024). Despite these advances, piston failures remain relatively common in internal combustion engines and are often associated with the combined effects of thermal loading, mechanical stresses, wear mechanisms, and abnormal combustion phenomena (Zhang et al., 2022). Typical failure modes include piston seizure, piston or piston rings fracture, piston pin damage, and increased lubricant consumption due to piston, piston rings, and cylinder liner wear (Ge et al., 2025; Pyrc et al., 2023). Furthermore, optimization techniques and numerical simulations have been applied to enhance piston durability and service life under severe operating conditions (Ghoujehzadeh et al., 2025; Kaliappan et al., 2020).

In addition to studies focusing on piston structural design, other studies have examined radiation heat transfer and friction phenomena in piston–cylinder assemblies to improve engine efficiency and durability (Bifeng et al., 2020; Yue and Reitz, 2019). These investigations provide an important foundation for comprehensively assessing piston operating conditions in modern engines. After conversion to CNG operation, engine operating parameters may change significantly. In this study, the maximum in-cylinder pressure and peak temperature increased by 37.44% and 2 %, respectively, compared with the original diesel operating condition. Such variations may considerably affect the operating environment and the durability of engine components, particularly the piston. Therefore, this study focuses on evaluating the piston's structural durability when the engine operates with CNG fuel.

2. Theoretical Background for Piston Thermal and Mechanical Load Analysis

To evaluate piston durability under engine operating conditions, both heat transfer mechanisms and mechanical loads acting on the component must be considered. This section presents the theoretical basis for heat transfer within the combustion chamber and the mechanical loading acting on the piston crown.

The energy exchange process in the combustion chamber is described based on the first law of thermodynamics, which reflects the principle of energy conservation. Accordingly, the energy released from fuel combustion is distributed into different forms, including the work output, the change in the internal energy of the working fluid, and the heat transferred to the combustion chamber walls. This principle forms the basis for analyzing heat transfer and evaluating thermal loads on engine components such as the piston, cylinder head, and cylinder liner, as given in Equation (1) (Bryden et al., 2022; Heywood, 2018):

$$\Delta U = Q - W \tag{1}$$

where:
ΔU : Change in the closed system's internal energy (kJ)
Q : Heat supplied to the system (kJ)
W : Work done by the system (kJ)

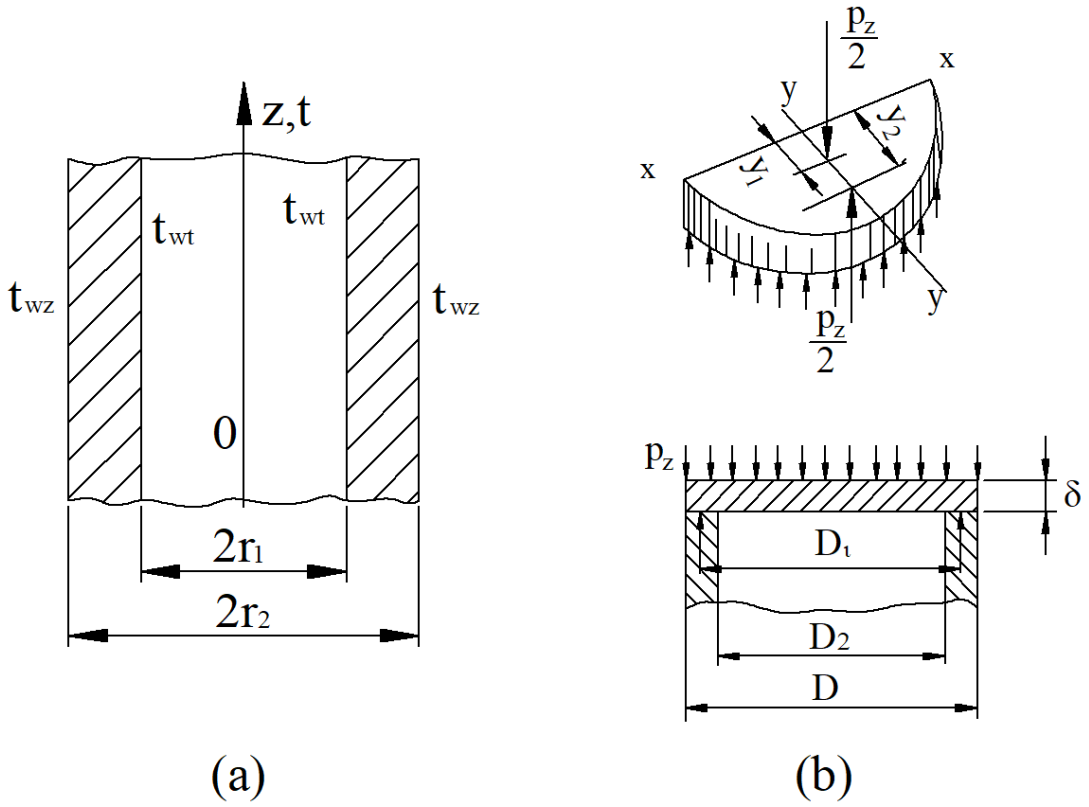

Figure 1 Models (Bryden et al., 2022): (a) Heat transfer through a single-layer cylindrical wall; (b) piston crown calculation

2.1 The heat transfer model

The convective heat transfer from the in-cylinder combustion gases to the combustion chamber components' surfaces is described by Equation (2) (Bryden et al., 2022; Heywood, 2018):

$$Q_{wi} = A_i \cdot \alpha_w (T_c - T_{wi}) \tag{2}$$

where:
Q_{wi} : Heat transferred to the wall (cylinder head, piston, and cylinder liner) (W)
A_i : Heat transfer area (cylinder head, piston, cylinder liner) (m^2)
α_w : Heat transfer coefficient (W/m^2K)
T_c : Temperature of the in-cylinder gas (K)
T_{wi} : Temperature of the wall (cylinder head, piston, cylinder liner) (K)

The heat from the combustion gases is first transferred to the inner surface by convection and then conducted through the material to the outer surface..For components with cylindrical geometry, such as the cylinder liner, the heat conduction process should be described using a single-layer cylindrical wall model, as expressed in Equation (3) (Bryden et al., 2022; Heywood, 2018): For heat transfer through a single-layer cylindrical wall, as illustrated in Figure 1(a), the heat flux is determined based on the following equation:

$$q_l = \frac{t_{w1} - t_{w2}}{\frac{1}{2\pi\lambda} \ln\left(\frac{d_2}{d_1}\right)} \tag{3}$$

where:
q_l : Heat flux per unit length transferred through the wall (W/m)
t_{w1}, t_{w2} : Temperatures at the inner and outer surfaces of the wall (K)
λ : Thermal conductivity of the wall material (W/m·K)
d_1, d_2 : Inner and outer diameters of the cylindrical wall, respectively (m)

2.2 Mechanical load analysis of the Piston

In addition to thermal loading, the piston is subjected to mechanical loading caused by the gas pressure in the combustion chamber, which plays a critical role in determining the piston crown's stress and deformation state. The piston crown experiences highly complex loading conditions involving both thermal and mechanical effects. Due to this complexity, finite element analysis is required to accurately evaluate the stress distribution on the piston crown.

In this study, the piston crown is modeled as a uniformly thick circular plate freely supported on a hollow cylinder, as shown in Figure 1(b). Gas pressure (p_x) acting on the piston crown is assumed to be uniformly distributed. This assumption is commonly adopted in piston structural analyses because the pressure waves inside the combustion chamber propagate much faster than the engine cycle's characteristic time scale, allowing the in-cylinder pressure to quickly approach a nearly uniform state. In addition, the relatively small combustion chamber volume and the strong turbulent motion of the working gases reduce local pressure gradients. Therefore, the gas pressure can be reasonably approximated as uniformly distributed over the piston surface for structural stress analysis of the piston crown (Bryden et al., 2022; Heywood, 2018). The resulting gas force is $P_z = p_x \cdot F_p$, which, together with the corresponding reaction force, causes piston crown bending.

3. Model Development

3.1 Research procedure

To evaluate the effects of switching to CNG on the engine piston by comparing the distributions of stress, deformation, and temperature when using diesel and CNG fuels, the piston loading analysis in this study was carried out using the finite element method within the SolidWorks Simulation environment according to the following procedure:

1. A three-dimensional geometric model of the piston based on the actual engine structure is constructed and imported into the simulation environment;
2. The material properties of the piston are defined according to the specifications of the manufacturing material;
3. The finite element mesh for the piston model is generated;
4. Boundary conditions and loads acting on the piston, including gas pressure acting on the piston crown, thermal loads, and constraints at the piston pin region, are applied;
5. The simulation was performed to determine the distributions of stress and deformation of the piston;
6. Comparison and analysis of the piston's stress and deformation results under the two fuel cases, CNG and Diesel.

3.2 Material and 3D model construction

3.2.1 Piston material

Owing to the characteristic thermal and mechanical loads acting on the piston of a diesel-fueled engine, the piston used in this study's engine is made of gray cast iron. The material properties of gray cast iron are presented in Table 1. The coefficient of thermal expansion, thermal conductivity, mechanical strength, density, and wear resistance are the primary properties usually considered when selecting piston material for internal combustion engines.

In the original engine configuration, the piston was manufactured from gray cast iron, which provides high mechanical strength and good wear resistance under the high pressure and temperature conditions typical of diesel combustion. This study aims to investigate the feasibility

of converting a diesel engine to operate on CNG for transportation applications. Modifications to the original engine structure were minimized to reduce the cost and complexity of practical implementation. Therefore, the original piston was retained. A minor modification was introduced by slightly reducing the piston crown height to adapt the engine to CNG operation and lower the compression ratio to a level suitable for CNG combustion.

Table 1 Mechanical properties of gray cast iron (Bryden et al., 2022; Heywood, 2018)

No	Properties	Value
1	Elastic modulus (GPa)	66.1
2	Yield strength (MPa)	315
3	Tensile strength (MPa)	152
4	Compressive strength (MPa)	572
5	Poisson's ratio	0.27
6	Thermal conductivity (W/m.K)	45
7	The thermal expansion coefficient (1/K)	1.2×10^{-5}
8	Density (kg/m^3)	7200

3.2.2 Piston specifications

The piston in the engine under study features a triangular combustion chamber. The specifications are illustrated in Table 2. Based on these parameters, the authors constructed the 3D model of the piston in SolidWorks for durability analysis. Figure 2(b) shows the 3D model of the engine piston.

Table 2 Main geometric parameters of the piston used in the simulation

No.	Parameter	Symbol	Size (mm)	Notes
1	Piston outer diameter	D	108	Piston crown
2	Total piston height	H	90	From crown to bottom
3	Piston skirt height	H_k	46	Piston skirt
4	Distance from crown to piston ring groove 1	–	20	Top ring groove
5	Distance from crown to piston ring groove 2	–	24	Second ring groove
6	Distance from crown to piston ring groove 3	–	28	Third ring groove
7	Distance from crown to piston ring groove 4	–	34	Fourth ring groove
8	Distance from crown to piston ring groove 5	–	36	Fifth ring groove
9	Height from base to piston tail	–	50	Piston bottom part
10	Piston pin hole	ϕ	10	4 holes around the axis

3.3 Calculation conditions

The original diesel engine has a compression ratio of 16.7. However, when converting the engine to operate on CNG, the compression ratio must be reduced to avoid knocking, which is more likely to occur with gaseous fuels at high compression ratios. According to previous studies, when operating on CNG, the engine compression ratio is typically adjusted to approximately 11 to limit knocking while still ensuring the required output power (Bryden et al., 2022; Heywood, 2018). In this study, to achieve the new compression ratio without modifying the main engine components, such as the cylinder head, the crankshaft–connecting rod mechanism, or the engine block, the authors selected the approach of reducing the piston crown height, thereby increasing the combustion chamber volume. The calculation results show that removing approximately $\Delta h = 5$ mm from the piston crown allows the engine to achieve the required combustion chamber volume and compression ratio when operating on CNG. When the engine operates at 2200 rpm,

the main parameters obtained include an engine power of Ne = 56.32 kW and a compression ratio of $\epsilon = 11$, ensuring stable engine operation after fuel conversion.

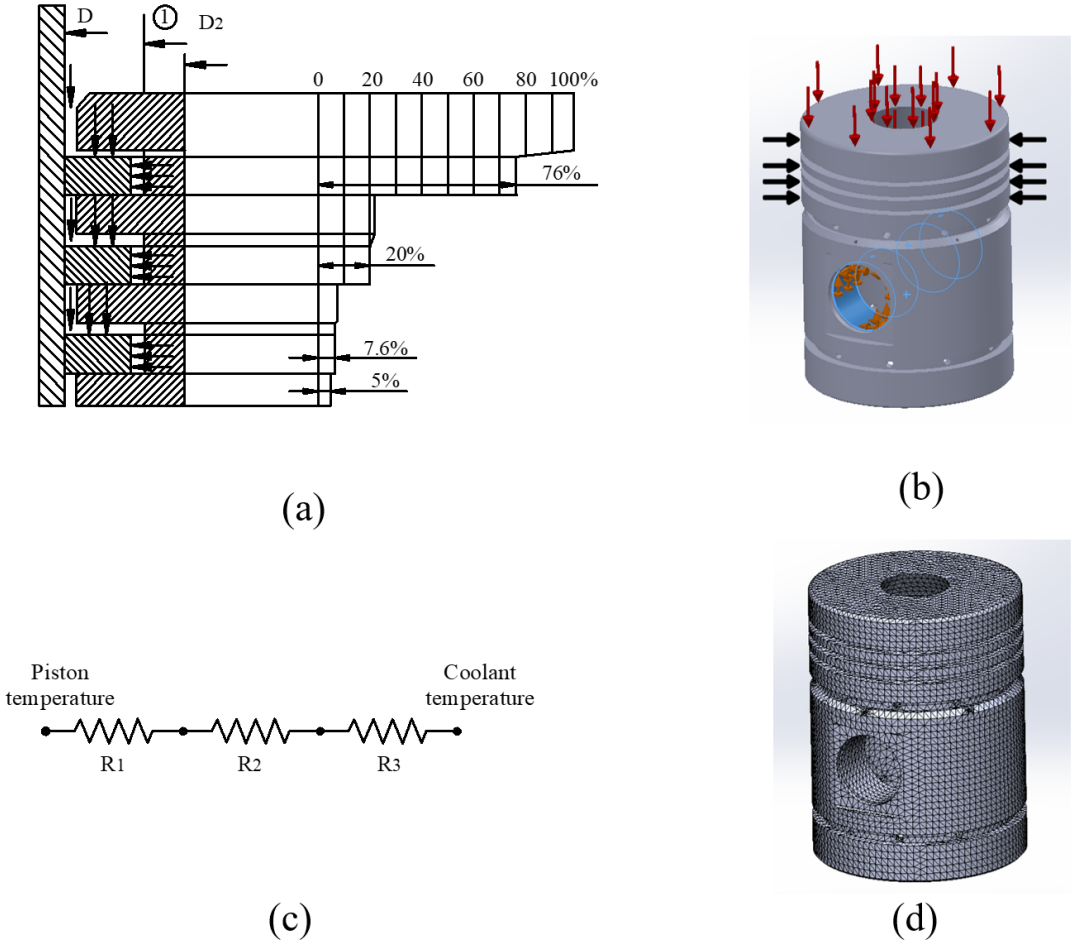

Figure 2 Load distribution on the piston: (a) pressure acting on the piston skirt, (b) piston boundary conditions under mechanical loading, (c) heat transfer model, and (d) piston meshing using the Meshing command

After adjusting the piston crown height, the compression ratio of the engine becomes 11, and the piston durability analysis is performed at this ratio. In this study, a model was developed to evaluate the thermomechanical stresses and deformations of the piston when operating with two types of fuel: diesel and CNG. Calculations are performed when the engine operates at full load and a speed of 2200 rpm.

For the mechanical loading case, the piston is assumed to be located at the top dead center (TDC), where the in-cylinder gas pressure acting on the piston crown reaches its maximum value (p_{zmax}). This position corresponds to the most critical loading condition for the piston because both the combustion pressure and the thermal load acting on the piston crown become significant during the combustion–expansion process.

The thermomechanical behavior of the piston is evaluated under this representative operating condition in the present study. Therefore, the time-dependent variation of pressure and temperature throughout the entire engine cycle (i.e., dynamic loading conditions) is not explicitly modeled as follows: The mechanical load is represented by the peak in-cylinder pressure acting on the piston crown. The thermal load is described by the heat transfer from the combustion gases to the piston surface. The heat transfer rate is estimated based on the method reported by Bryden et al., 2022 as follows.

This approach allows a clear comparison of the piston's temperature distribution, thermal stress, and deformation when the engine operates with diesel and CNG fuels while maintaining the computational model at a reasonable level of complexity. For the thermal loading case,

the simulation was also conducted with the piston positioned at the TDC during the combustion–expansion process. At this moment, combustion occurs inside the combustion chamber, and a portion of the released heat is transferred to the piston crown. After establishing the model, this study evaluates the thermal effects by comparing the piston temperature distribution and thermal stress under diesel and CNG operating conditions. For the combined thermomechanical loading case, both mechanical stress and thermal loads are applied simultaneously to examine their combined effects on the piston structure when operating with the two different fuels.

3.4 Boundary conditions

3.4.1 Boundary conditions under mechanical loading conditions

When calculating the mechanical load on the piston, the authors apply the maximum cylinder pressure, (p_{zmax}) acting perpendicularly to the piston crown surface, representing the primary mechanical load on the piston. In addition, some of the working fluid escapes into the crankcase through clearances between the piston, cylinder wall, and compression rings due to blow-by in the combustion chamber. Therefore, the side surface of the piston is also subjected to gas pressure (Figure 2(a)) (Bryden et al., 2022; Heywood, 2018).

The boundary conditions of the piston under mechanical loading are presented in Figure 2(b). In the numerical model, the piston pin bore surface is fixed to represent the constraint between the piston and the connecting rod. To better highlight the effect of gas pressure and simplify the computational model, other mechanical loads, such as lateral and friction forces, are assumed to be negligible when the piston is located at the top dead center.

In addition, in the vicinity of TDC, where the combustion pressure reaches its peak value, the inertia force generally acts in the opposite direction to the gas force and partially reduces the mechanical load acting on the piston. However, in this study, the influence of inertia forces is neglected to focus on the effect of combustion gas pressure on the piston.

The maximum cylinder pressure used in the calculations is $p_{zmax} = 6.758$ (MPa) for the piston operating with diesel fuel, whereas for the piston operating with CNG, the maximum cylinder pressure is $p_{zmax} = 3.847$ (MPa).

3.4.2 Boundary conditions under thermal loading conditions

Heat transfer in the engine consists of two main types: heat transferred into and out of the components. The piston crown absorbs a portion of the released heat, while the coolant transfers the remaining heat through the combustion chamber walls. After entering the piston via the crown, most of the heat is directed to the coolant through the piston rings. Another portion is transferred from the inner piston surfaces to the surrounding air, and the rest flows through the piston pin surfaces to the connecting rod and crankshaft. The coolant is modeled by assigning a convective heat transfer coefficient of water to all piston surfaces in contact with the cooling jacket.

Heat is transferred into the piston crown as follows:

The heat directly transferred from the combustion gases to the piston crown represents the main thermal load acting on the piston. The heat input to the piston is calculated using Equation (4) (Bryden et al., 2022).

$$H = K \cdot C \cdot m \cdot N_{hp} \tag{4}$$

where:

H : Heat transferred through the piston crown (kW); for the engine fueled with diesel and CNG, the value of H is 1.903 (kW)

K : Percentage of heat absorbed by the piston crown, ranging from 4% to 5.25%. In the present work, the coefficient K was introduced into the model with values of $K = 4.23\%$ for diesel fuel and $K = 4.45\%$ for CNG

C : Lower heating value of the fuel; 42700 kJ/kg for diesel and 50000 kJ/kg for CNG
m : Fuel mass flow rate (kg/kW.s)
N_{hp} : Brake power per cylinder (kW)

Heat transfer through the piston rings:

In this region, the heat transmitted from the piston crown is conducted through the piston rings, the cylinder liner, and finally to the coolant, as illustrated in Figure 2(c) (Bryden et al., 2022; Subbarao and Gupta, 2020). To model this process, the authors employed the thermal–resistance network method with the following assumptions:

- Heat transfer through the piston rings is conduction through a multilayer cylindrical wall.
- The environment surrounding the piston is assumed to be coolant water with a uniform temperature of 100°C (373 K).
- The influence of piston motion on heat transfer is neglected.
- Ring rotation is not considered.
- The thermistor value is: $R_1 = 0.0867$ m^{2}K/W, $R_2 = 0.002$ m^{2}K/W, $R_3 = 0.005$ m^{2}K/W.

Heat transfer through the piston skirt:

In this region, the convective heat-transfer coefficient is 115 W/m^{2}K, with a coolant temperature of 373 K (Ambarev and Taneva, 2025; Bryden et al., 2022).

Heat transfer through the inner piston surfaces:

Since the inner surfaces of the piston (including the lower face of the crown and the inner surface of the skirt) are cooled by air, the convective heat-transfer coefficient is taken as 25 (W/m^{2}K), with an ambient air temperature of 397 (K) (Yang et al., 2022; Heywood, 2018).

Heat transfer through the piston pin bore:

The convective heat-transfer coefficient for this surface is 1000 W/m^{2}K, with an ambient temperature of 397 K (Liu et al., 2022; Heywood, 2018). Table 3 summarizes the heat-transfer coefficients for all piston surfaces.

3.5 Model construction and meshing

The finite element method (FEM) is a widely used numerical approximation technique for solving problems described by partial differential equations over a defined domain with arbitrary geometry and boundary conditions, where an exact analytical solution is not feasible.

The FEM is based on discretizing the problem domain into smaller subdomains called elements, which are connected at common nodes. Within each element, the solution is approximated by a selected function defined in terms of unknown values at the nodes, called shape functions, which satisfy the element's equilibrium conditions. Considering all elements together and enforcing the continuity of displacements and deformations at the shared nodes leads to a linear algebraic equation system. Solving this system provides the approximate solution values at all nodes, allowing the approximate function to be fully determined across each element. In this study, FEM was used to accurately simulate the mechanical and thermal loads acting on the piston using SolidWorks Simulation.

After creating the 3D piston model, it was imported into the simulation module to perform structural and thermal analyses. The piston geometry was then discretized using the FEM with a curvature-based meshing technique. Mesh density is an important parameter that affects numerical simulation accuracy and convergence. Therefore, to ensure that the simulation results are independent of the mesh density, a mesh convergence study was conducted by testing several mesh configurations with different numbers of elements and computational nodes. The maximum piston stress was selected as the convergence criterion for evaluating the numerical solution. Based on the convergence analysis, an element size ranging from 0.8 mm to 4 mm was selected

for the final simulations (Figure 2(d)). The piston model operating with diesel fuel consisted of 157888 elements and 240657 nodes after meshing, whereas the piston model operating with CNG consisted of 143086 elements and 218214 nodes. The key simulation outputs, such as piston temperature distribution and stress fields, show only negligible variations under these mesh configurations compared with those obtained using neighboring mesh densities. Therefore, the selected mesh configuration provides a reasonable balance between computational accuracy and computational cost while ensuring reliable predictions of the piston stress, deformation, and thermal distribution.

After meshing, the simulation is run to evaluate the results. The software sequentially computes the solution for each element using finite element algorithms, and this process may take several minutes.

4. Results and Discussion

4.1 Effect of the mechanical loading

Figures 3(a) and 3(b) present the simulation results of the piston mechanical stress distribution for the two fuels are presented in Figure 3(a) and Figure 3(b). When the engine operates on diesel fuel, the maximum mechanical stress on the piston reaches 125 MPa, whereas for the CNG-fueled engine, the maximum stress is only 68.23 MPa, corresponding to a significant reduction of approximately 45%. This trend is consistent with previous studies indicating that natural gas–based engines generally exhibit lower peak combustion pressures due to their lower compression ratios and smoother combustion characteristics compared to diesel engines (Abdullah and Abedin, 2024; Song et al., 2024; Shao et al., 2024).

The mechanical load acting on the piston induces deformation over the entire piston structure, with the most pronounced deformation concentrated at the central region of the piston crown (Figures 3(c) and 3(d)). This deformation pattern agrees well with reported numerical and experimental investigations on piston structural behavior, where the piston crown is identified as the primary load-bearing zone subjected to gas pressure forces (Ambarev and Taneva, 2025; Jiao et al., 2023; Roychoudhury et al., 2021). The maximum mechanical deformation of the diesel-fueled piston is 0.048 mm, which is considerably higher than that of the CNG-fueled piston (0.027 mm), representing a reduction of 43.75%. This reduction in mechanical stress and deformation indicates an increased safety margin for piston operation under CNG conditions. It also indicates the potential for optimizing piston design by reducing mass, which can improve engine efficiency and dynamic performance.

The observed reduction in both mechanical stress and deformation for the CNG case can be primarily attributed to the lower compression ratio of the CNG engine compared with that of the diesel engine (11 versus 16.7). A lower compression ratio reduces the maximum in-cylinder pressure (pzmax) during combustion, thereby decreasing the mechanical loading applied to the piston crown (Tien and Tuan, 2026; Kiran et al., 2020). Similar conclusions have been reported in previous studies (Wakshume and Sufe, 2025; Sharma et al., 2021), which emphasized the dominant role of peak cylinder pressure in governing piston mechanical integrity.

4.2 Effect of the thermal loading

Figures 4(a) and 4(b) show the simulated piston temperature distributions for the diesel and CNG engines are illustrated in Figure 4(a) and Figure 4(b). The results reveal that the maximum piston temperature in the diesel engine reaches 380.5°C, whereas the CNG-fueled piston experiences a significantly higher peak temperature of 420°C, corresponding to an increase of approximately 10%. This increase in temperature may accelerate material degradation, reduce fatigue life, and increase the risk of piston seizure under high-load operating conditions. This behavior is mainly attributed to the higher heating value and cleaner combustion of CNG, which leads to increased heat release and enhanced thermal loading on the piston surface (Yang et al., 2024; Liu et al., 2022; Subbarao and Gupta, 2020).

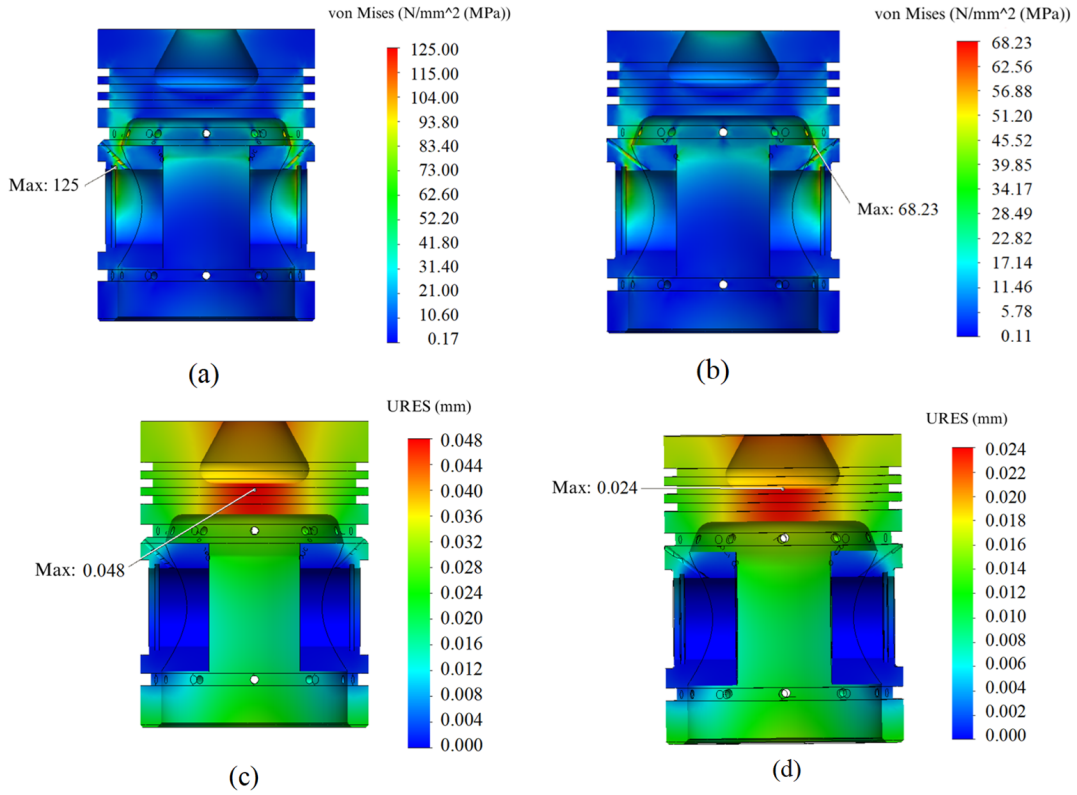

Figure 3 Effects of mechanical load on piston mechanical stress distribution for (a) diesel and (b) CNG and on piston mechanical deformation for (c) diesel and (d) CNG

Although the higher heat release associated with CNG combustion can enhance engine efficiency and power output, it also imposes more stringent thermal management requirements on the piston. Elevated temperature levels intensify thermal gradients within the piston structure, which can affect dimensional stability and alter the stress distribution during operation (Apaydin and Doner, 2024; Pastor et al., 2021). As a result, ensuring effective heat dissipation and optimizing piston design, including material selection and cooling strategies, are essential for maintaining reliable performance under CNG operating conditions.

The thermal stress distributions of the piston for both fuels are shown in Figures 4(c) and 4(d). The results indicate that the maximum thermal stress in the diesel-fueled piston is 257.1 MPa, whereas the CNG-fueled piston experiences a higher value of 271.3 MPa, representing an increase of approximately 5%. Although this increase is moderate, it may have a significant impact on long-term durability, especially under cyclic TM loading conditions. This increase is directly associated with the higher temperature gradients induced by CNG combustion, which intensify thermally induced stresses within the piston material (Zhang et al., 2024; Abdullah and Abedin, 2024).

Figures 4(e) and 4(f) present the simulated thermal deformation of the piston under both fuel conditions. The maximum thermal deformation for the diesel-fueled piston is 0.227 mm, whereas it increases to 0.236 mm for the CNG-fueled piston, corresponding to a 4% increase. The increase in thermal deformation may influence the piston–cylinder clearance, potentially resulting in higher friction, increased wear, and reduced engine reliability. The findings confirm that the elevated operating temperature of the CNG-fueled piston leads to greater thermal expansion, thereby intensifying both thermal stress and deformation levels (Jiao et al., 2023; Sharma et al., 2021).

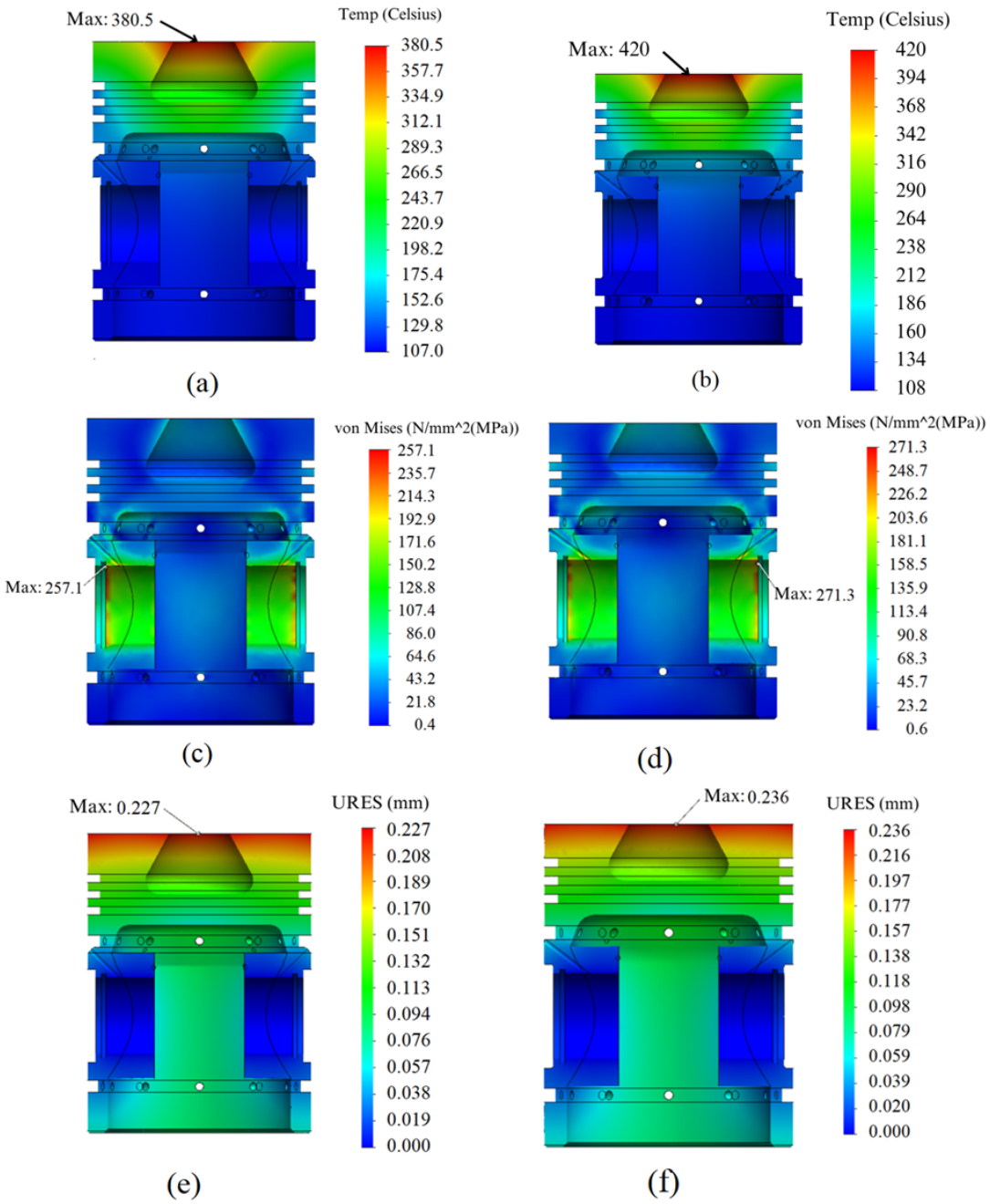

Figure 4 Effects of thermal load on piston temperature distribution for diesel (a) and CNG (b), thermal stress distribution for diesel (c) and CNG (d), and piston thermal deformation for diesel (e) and CNG (f)

4.3 Simulation results of piston under combined mechanical and thermal loading

The combined effects of mechanical and thermal loading on piston stress distribution for both fuels are shown in Figures 5(a) and 5(b). The simulation results demonstrate that the maximum combined stress for the diesel-fueled piston reaches 317 MPa, whereas it is reduced to 301.5 MPa for the CNG-fueled piston, corresponding to a decrease of approximately 5%. The results indicates that operating with CNG enhances the piston's structural safety, while the primary design consideration shifts from mechanical strength toward thermal resistance. The observed reduction further implies that although CNG combustion leads to higher thermal stresses, the significant decrease in mechanical loading predominates in reducing the overall stress level (Wakshume and Sufe, 2025; Mishra et al., 2023; Liu et al., 2022).

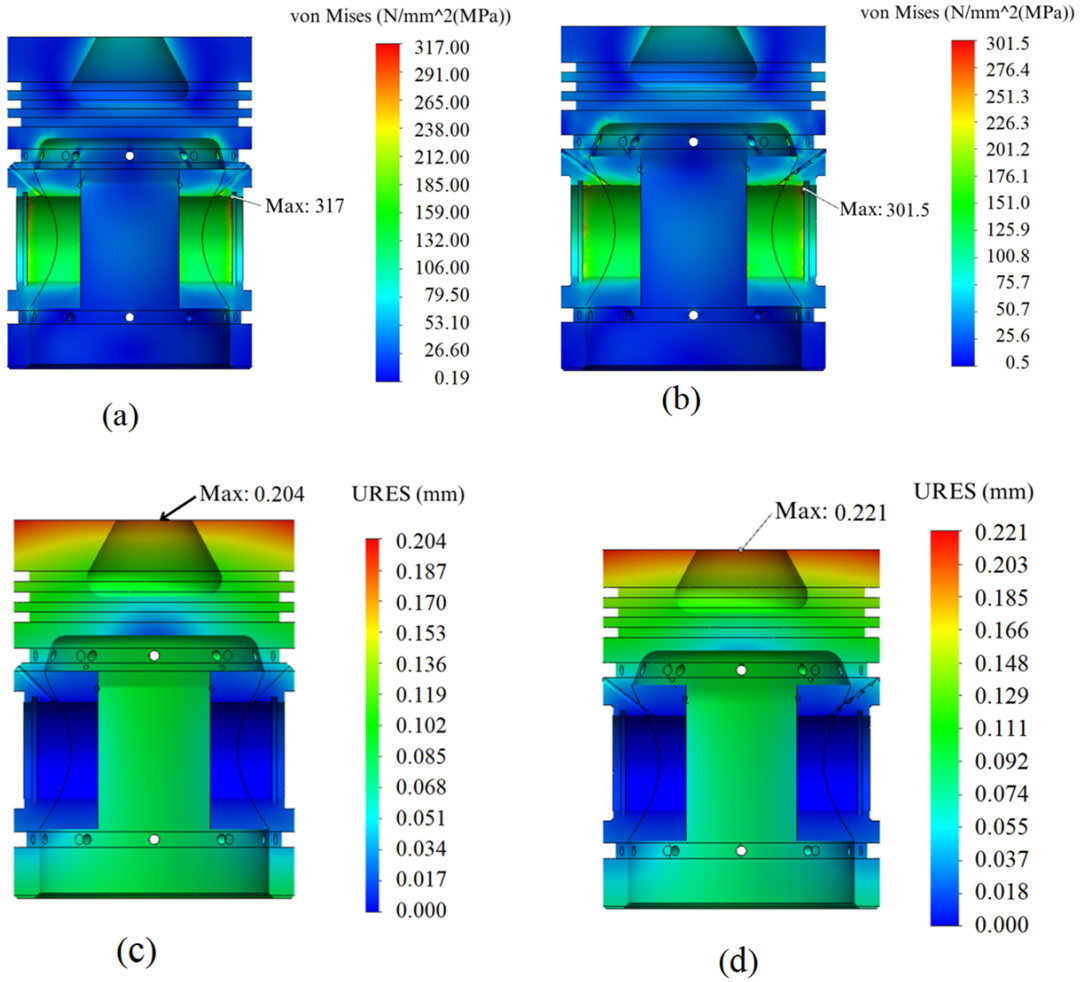

Figure 5 Effects of combined mechanical and thermal loads on the mechanical–thermal stress distribution of the engine piston for diesel (a) and CNG (b), and on the mechanical–thermal deformation of the engine piston for diesel (c) and CNG (d)

Figures 5(c) and 5(d) show the combined mechanical and thermal deformation results. The maximum deformation of the diesel-fueled piston is 0.204 mm, whereas the CNG-fueled piston exhibits a higher deformation of 0.221 mm, corresponding to an 8% increase. The increase in deformation highlights the dominant role of thermal effects and indicates the need for improved piston design thermal management strategies. This finding highlights that thermal deformation becomes the governing factor for piston dimensional stability in CNG-fueled engines, even when the combined stress level is lower than that of diesel engines (Apaydin and Doner, 2024; Roychoudhury et al., 2021).

Overall, the combined loading analysis indicates that while CNG operation improves piston mechanical safety by reducing peak stress levels, it simultaneously increases the risk of excessive deformation due to elevated thermal loads. Therefore, optimized piston design, improved cooling strategies, and appropriate material selection are essential to ensure reliable operation of CNG-fueled engines under combined mechanical and thermal loading conditions (Song et al., 2024; Yang et al., 2024). The simulation results for all cases are summarized in Table 3.

Table 3 presents a comparison of the changes in engine technical characteristics when using CNG compared to diesel. The blue color with a downward arrow indicates a decreasing trend, whereas the red color with an upward arrow indicates an increasing trend. The results presented in Table 3 show that the mechanical load acting on the piston is significantly reduced when the engine operates with CNG fuel compared with diesel operation. Specifically, the maximum mechanical stress decreased from 125 to 68.23 MPa (a reduction of approximately 45%), while

the mechanical deformation decreased from 0.048 to 0.027 mm (a reduction of approximately 43.75%). This decrease in mechanical loading increases the piston's structural safety margin and improves its durability and service life. From an engineering perspective, these results indicate that while CNG fuel reduces mechanical loading on the piston, it significantly increases thermal loading. Therefore, piston design for CNG engines should prioritize enhanced cooling strategies, improved thermal resistance, and materials with lower thermal expansion coefficients.

Table 3 Summary of simulation results

Load Type		*Diesel*	*CNG*	
Mechanical	Stress (MPa)	125	68.23	↓45%
	Deformation (mm)	0.048	0.027	↓43.75%
Thermal	Temperature (°C)	380.5	420	↑10%
	Stress (MPa)	257.1	271.3	↑5%
	Deformation (mm)	0.227	0.236	↑4%
Mechanical + Thermal	Stress (MPa)	317	301.5	↓5%
	Deformation (mm)	0.204	0.221	↑8%

Furthermore, the lower mechanical load indicates a potential opportunity for piston design optimization in future studies. With further structural verification, the piston crown thickness could potentially be reduced to decrease the reciprocating mass and improve the engine's dynamic performance. However, increased thermal loading leads to a significant rise in piston temperature during operation, resulting in greater thermal deformation. This deformation may alter the piston-to-cylinder clearance, potentially increasing friction and the risk of piston seizure, while also reducing structural rigidity and strength under operating conditions.

5. Conclusions

This study investigated the effects of mechanical loading, thermal loading, and their combined thermo-mechanical interaction on the piston when converting an engine from diesel to CNG using numerical simulation. The results indicate that under CNG operation, both mechanical stress and deformation of the piston decrease significantly, by approximately 45% and 43.75%, respectively, compared to diesel conditions. However, the piston temperature increases by approximately 10%, leading to corresponding increases of approximately 5% in thermal stress and 4% in thermal deformation. When both loading types are considered simultaneously, the overall stress shows a slight reduction of approximately 5%, whereas the total deformation increases by approximately 8%, suggesting that thermal effects become the dominant factor influencing piston durability under CNG conditions. Although the resulting stress levels remain within the material strength limits, the findings emphasize the importance of effective thermal management, appropriate material selection, and optimized piston design to ensure reliable engine performance. Nevertheless, this study has certain limitations, as it considers only a representative operating condition and does not fully account for dynamic effects, friction, or TM fatigue. Therefore, future work should extend the analysis to full engine-cycle simulations, incorporate CFD-based combustion modeling, and include experimental validation to achieve a more comprehensive assessment of piston durability in CNG-fueled engines.

Author Contributions

Nguyen Van Tuan: Writing – review & editing, Methodology, Data curation, Writing – original draft, Investigation, Supervision, Conceptualization, Data curation.

Nguyen Duy Tien: Writing – original draft, Validation, Writing – review & editing, Visualization, Investigation.

Conflict of Interest

The authors declare that they have no known competing financial interests or personal relationships that could have appeared to influence the work reported in this paper.

References

Abdullah, M., & Abedin, M. Z. (2024). Recent development of combined heat transfer performance for engine systems: A comprehensive review. *Results in Surfaces and Interfaces*, *15*, 100212. https://doi.org/10.1016/j.rsurfi.2024.100212

Ali, Y., Younus, A., Khan, A. U., & Alrefai, A. H. (2024). Compressed natural gas (CNG) as a fuel and the associated risks: A quantitative analysis in the scenario of a developing country. *Safety Science and Resilience*, *5*, 306–316. https://doi.org/10.1016/j.jnlssr.2024.05.001

Ambarev, K., & Taneva, S. (2025). Thermal and structural analysis of gasoline engine piston at different boost pressures. *Engineering Proceedings*, *100*(1), 38. https://doi.org/10.3390/engproc2025100038

Apaydin, S., & Doner, N. (2024). Effects of piston cooling gallery geometry on temperature and flow in a heavy-duty diesel engine. *Thermal Science and Engineering Progress*, *51*, 102644. https://doi.org/10.1016/j.tsep.2024.102644

Bifeng, Y., Jiajun, Z., Bo, X., & et al. (2020). Friction and wear performance of a double-bump piston skirt design on the main thrust side. *International Journal of Automotive Technology*, *21*(6), 1579–1586. https://doi.org/10.1007/s12239-020-0148-y

Bryden, K., Ragland, K. W., & Kong, S. C. (2022). *Combustion engineering*. CRC Press.

Chen, H., Hofbauer, P., & Longtin, J. P. (2020). Multi-objective optimization of a free-piston Vuilleumier heat pump using a genetic algorithm. *Applied Thermal Engineering*, *167*, 114767. https://doi.org/10.1016/j.applthermaleng.2019.114767

Cihan, O., Doğan, H. E., Kutlar, O. A., Demirci, A., & Javadzadehkalkhoran, M. (2020). Evaluation of heat release and combustion analysis in spark ignition Wankel and reciprocating engines. *Fuel*, *261*, 116479. https://doi.org/10.1016/j.fuel.2019.116479

Du, Y., Fei, C., Qian, Z., Zhu, S., Shu, Z., & Zhou, K. (2024). Simulation analysis of thermal insulation performance of diesel engine piston based on PEO and $La_2Zr_2O_7$ thermal barrier coating. *Case Studies in Thermal Engineering*, *59*, 104460. https://doi.org/10.1016/j.csite.2024.104460

Ge, C., Zhang, B., Xu, X., Lyu, X., Ma, X., Li, T., Lu, X., & Liu, Z. (2025). Tribofilm distribution and tribological analysis of piston ring–cylinder liner interfaces under realistic engine conditions. *Tribology International*, *201*, 110250. https://doi.org/10.1016/j.triboint.2024.110250

Ghoujehzadeh, A., Bonab, M. A. M., & Jahani, D. (2025). Optimization and finite element analysis of an aluminum piston in the Peugeot XU7JPL3 engine for enhanced efficiency and durability. *Discover Mechanical Engineering*, *4*(1), 1–18. https://doi.org/10.1007/s44245-025-00091-w

Heywood, J. B. (2018). *Internal combustion engine fundamentals* (2nd edn). McGraw-Hill Education.

Jiao, B., Ma, X., Wang, Y., Lyu, X., Li, T., & Liu, Z. (2023). A fluid-structure coupled transient mixed lubrication model for piston ring lubrication property analysis. *International Journal of Mechanical Sciences*, *252*, 108377. https://doi.org/10.1016/j.ijmecsci.2023.108377

Kaliappan, S., Mohanamurugan, S., & Nagarajan, P. K. (2020). Numerical investigation of sinusoidal and trapezoidal piston profiles for an internal combustion engine. *Journal of Applied Fluid Mechanics*, *13*(1), 287–298. https://doi.org/10.29252/jafm.13.01.29881

Karczewski, M., & Wieczorek, M. (2021). Assessment of the impact of a non-factory diesel/natural gas dual-fuel system on traction performance and exhaust emissions of a semi-trailer truck. *Energies*, *14*(23), 8001. https://doi.org/10.3390/en14238001

Kiran, S., Palanivendhan, M., & Kumar, M. (2020). Modelling and analysis of piston and piston rings of SI engine for different materials using FEM. *IOP Conference Series: Materials Science and Engineering*, *993*, 1–16. https://doi.org/10.1088/1757-899X/993/1/012155

Kundu, S., & Gupta, H. (2024). Combustion and emission characteristics of CNG/gasoline direct fuel injection engines. *Fuel*, *359*, 130537. https://doi.org/10.1016/j.fuel.2023.130537

Kyando, M. J., Ntalikwa, J. W., & Kivevele, T. (2026). Compressed natural gas in aged internal combustion engines: performance, emissions, and challenges – a systematic review. *Energy Conversion and Management: X*, *30*, 101726. https://doi.org/10.1016/j.ecmx.2026.101726

Lei, J., Xu, S., Liu, Y., Deng, X., Tang, A., & Lin, D. (2024). Multi-objective optimisation of heat transfer and structural strength of aero-piston air-cooled engine cylinder based on orthogonal test. *Thermal Science and Engineering Progress*, *50*, 102500. https://doi.org/10.1016/j.tsep.2024.102500

Liu, B., Aggarwal, S. K., Zhang, S., Tchakam, H. U., & Luo, H. (2023). Thermo-mechanical coupling strength analysis of a diesel engine piston based on finite element method. *International Journal of Green Energy*, *21*(4), 732–744. https://doi.org/10.1080/15435075.2023.2211139

Liu, Y., Jing, G., Liu, H., Zhang, W., Han, M., Xiao, S., & Zhang, Z. (2022). Failure analysis and design improvements of steel piston for a high-power marine diesel engine. *Engineering Failure Analysis*, *142*, 106825. https://doi.org/10.1016/j.engfailanal.2022.106825

Meng, X., Tian, H., Long, W., Zhou, Y., Bi, M., Tian, J., & Lee, C.-F. (2019). Experimental study on the use of additives in pilot fuel for performance and emission trade-offs in diesel/CNG dual-fuel combustion. *Applied Thermal Engineering*, *157*, 113718. https://doi.org/10.1016/j.applthermaleng.2019.113718

Mishra, P. C., Roychoudhury, A., Banerjee, A., Saha, N., Das, S. R., & Das, A. (2023). Coated piston ring pack and cylinder liner elastodynamics in correlation to piston subsystem elastohydrodynamic: through FEA modelling. *Lubricants*, *11*, 192. https://doi.org/10.3390/lubricants11050192

Nsaif, O., Kokjohn, S., Hessel, R., & Dempsey, A. (2024). Reducing methane emissions from lean burn natural gas engines with prechamber ignited mixing-controlled combustion. *Journal of Engineering for Gas Turbines and Power*, *146*, 061023. https://doi.org/10.1115/1.4064454

Pastor, J. V., García, A., Micó, C., Lewiski, F., Vassallo, A., & Pesce, F. C. (2021). Effect of a novel piston geometry on the combustion process of a light-duty compression ignition engine: an optical analysis. *Energy*, *221*, 119764. https://doi.org/10.1016/j.energy.2021.119764

Plotnikov, L. (2024). Gas dynamics and heat exchange of stationary and pulsating air flows during cylinder filling process through different configurations of the cylinder head channel. *International Journal of Heat and Mass Transfer*, *233*, 126041. https://doi.org/10.1016/j.ijheatmasstransfer.2024.126041

Pyrc, M., Gruca, M., & Tutak, W. (2023). Assessment of the co-combustion process of ammonia with hydrogen in a research variable compression ratio piston engine. *International Journal of Hydrogen Energy*, *48*(6), 2821–2834. https://doi.org/10.1016/j.ijhydene.2022.10.152

Qi, J., Dong, Y., Liu, J., Li, H., Liu, Y., & Zhang, S. (2021). Analysis and optimization study of piston in diesel engine based on ABC-OED-FE method. *Mathematical Problems in Engineering*, *2021*, 3205695. https://doi.org/10.1155/2021/3205695

Roychoudhury, A., Banerjee, A., Mishra, P. C., & Khoshnaw, F. (2021). An FEA material strength modelling of a coated engine piston. *Materials Today: Proceedings*, *44*, 1320–1325. https://doi.org/10.1016/j.matpr.2020.11.387

Sadiq, Y. R., & Iyer, R. C. (2020). Experimental investigation on the influence of compression ratio and piston crown geometry on the performance of a biogas-fueled spark ignition engine. *Renewable Energy*, *146*, 997–1009. https://doi.org/10.1016/j.renene.2019.06.140

Shao, L., Zhou, Y., Geng, T., Zhao, S., Zhu, K., Zhong, Z., Yan, H., Yu, T., Xu, Z., & Ding, S. (2024). Advanced combustion in heavy fuel aircraft piston engines: A comprehensive review and future directions. *Fuel*, *370*, 131771. https://doi.org/10.1016/j.fuel.2024.131771

Sharma, J. K., Raj, R., Kumar, S., Jain, R. K., & Pandey, M. (2021). Finite element modeling of lanthanum cerate coated piston used in a diesel engine. *Case Studies in Thermal Engineering*, *25*, 100865. https://doi.org/10.1016/j.csite.2021.100865

Shen, Z., Wang, X., Zhao, H., Lin, B., Shen, Y., & Yang, J. (2021). Numerical investigation of a natural gas–diesel dual-fuel engine with different piston geometries and radial clearances. *Energy*, *220*, 119706. https://doi.org/10.1016/j.energy.2020.119706

Song, J., Gao, J., Gharehghani, A., Gao, J., Huang, Y., Wang, X., Wang, Y., Fu, Z., Qi, M., & Tian, G. (2024). Research on the in-cylinder combustion and emissions of opposed rotary piston engines over various altitudes. *Fuel*, *376*, 132644. https://doi.org/10.1016/j.fuel.2024.132644

Subbarao, R., & Gupta, S. (2020). Thermal and structural analyses of an internal combustion engine piston with suitable different super alloys. *Materials Today: Proceedings*, *22*, 2950–2956. https://doi.org/10.1016/j.matpr.2020.03.429

Tien, N. D., & Tuan, N. V. (2026). Research on the technical and economic performance and emissions of diesel engines when converted to compressed natural gas fuel. *Cleaner Energy Systems*, 100248. https://doi.org/10.1016/j.cles.2026.100248

Wakshume, E., & Sufe, G. (2025). Finite element analysis of engine pistons: comparative assessment of aluminium and titanium alloys under combined thermal-structural loading. *Scientific Reports*, *15*, 41593. https://doi.org/10.1038/s41598-025-25473-8

Wang, Q., Wu, F., Zhao, Y., Bai, J., & Huang, R. (2019). Study on combustion characteristics and ignition limit extension of micro free-piston engines. *Energy*, *179*, 805–814. https://doi.org/10.1016/j.energy.2019.05.003

Yang, F., Feng, H., Zhang, Z., Wu, L., & Wang, J. (2024). Effect of key parameter on the energy consumption and start-up time in the cold start-up process of an opposed-piston free-piston linear generator. *Applied Thermal Engineering*, *252*, 123441. https://doi.org/10.1016/j.applthermaleng.2024.123441

Yang, L., Lei, J., Wang, D., Deng, X., Wen, J., & Wen, Z. (2022). Experimental and simulation study on heat transfer characteristics of aluminium alloy piston under transition conditions. *Scientific Reports*, *12*, 9262. https://doi.org/10.1038/s41598-022-13357-0

Yousefi, A., Guo, H., & Birouk, M. (2019). Effects of diesel injection timing on combustion characteristics of a natural gas/diesel dual-fuel engine under low and high load and speed conditions. *Fuel*, *235*, 838–846. https://doi.org/10.1016/j.fuel.2018.08.064

Yue, Z., & Reitz, R. (2019). Numerical investigation of radiative heat transfer in internal combustion engines. *Applied Energy*, *235*, 147–163. https://doi.org/10.1016/j.apenergy.2018.10.098

Zhang, G., Huang, Z., & Li, G. (2024). Transient heat transfer and deformation characteristics of a bidirectional compressor cylinder block–piston assembly under multi-field coupling. *Applied Thermal Engineering*, *247*, 123083. https://doi.org/10.1016/j.applthermaleng.2024.123083

Zhang, T., Eismark, J., Münch, K., & Denbratt, I. (2019). Effects of wave-shaped piston bowl geometry on the performance of heavy-duty diesel engines fueled with alcohols and biodiesel blends. *Renewable Energy*, *148*, 1164–1175. https://doi.org/10.1016/j.renene.2019.10.057

Zhang, Z., Feng, H., Jia, B., Zuo, Z., Yan, X., Smallbone, A., & Roskilly, A. P. (2022). Identification and analysis on the variation sources of a dual-cylinder free-piston engine generator. *Energy*, *242*, 123001. https://doi.org/10.1016/j.energy.2021.123001